

黄海漂浮藻类光谱特征分析及鉴别研究

安德玉^{1, 2}, 邢前国^{1, 2*}, 李琳¹, 孟灵^{1, 2}

(1 中国科学院烟台海岸带研究所, 山东, 烟台 264003; 2 中国科学院大学, 北京 100049)

摘要 近年, 由浒苔爆发引起的绿潮及由马尾藻爆发引发的金潮均在我国以黄海、东海海域为主的近海海域出现(Xing *et al*, 2017), 对海洋生态环境、经济和人类生活产生了很大影响。漂浮藻类光谱特征是利用遥感手段监测藻类分布信息的重要基础, 本研究于 2017 年 6 月 9 日 ~ 2017 年 6 月 19 日, 在 33° 37' ~ 36° 30' N 和 120° 00' ~ 123° 30' E 的黄海海域内, 共采集浒苔和马尾藻样本 10 份样本, 利用光纤光谱仪和多光谱成像仪对其进行光谱采集。光纤光谱仪采集的高光谱数据用于进行光谱特征, 多光谱成像仪采集的数据尝试利用阈值法和神经网络方法区分浒苔和马尾藻。

本研究中, 计算虚拟基线漂浮藻类指数 (VB-FAH), 用于提取藻类信息; 基于反射谷深度 (T-Depth) 和虚拟基线漂浮藻类指数 (VB-FAH), 设置合理的阈值进行藻类区分 (邢前国等, 2013; Xing *et al*, 2016)。如果一个像元的 T-depth 值大于 0.295 或者 VB-FAH 值大于 0.4375, 则该像元被认为是浒苔。针对神经网络方法, 采用了三种数据进行分类, 分别是多光谱反射率图像 (Image_R)、多光谱反射率与 T-depth 组合图像 (Image_{R+T-depth})、多光谱反射率与 VB-FAH 组合图像 (Image_{VB-FAH})。最后, 对三种图像的神经网络分类效果进行比较。

Table 1 Sampling records

Floating macroalgae	Samples
<i>Sargassum</i>	01、04、05、06
<i>Ulva prolifera</i>	02、03、07、08、09、10

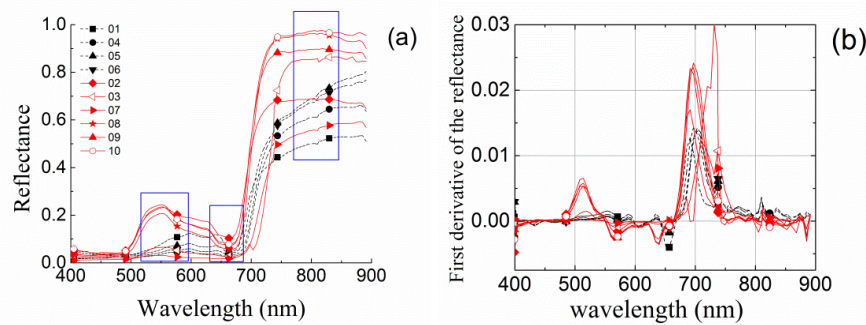


Fig.1. (a) The hyperspectral reflectance of floating macroalgae; (b) First derivative of the spectral reflectance. The red and black lines represents the *Ulva prolifera* and the *Sargassum*, respectively. The blue frame represents the corresponding band range of the multispectral imager.

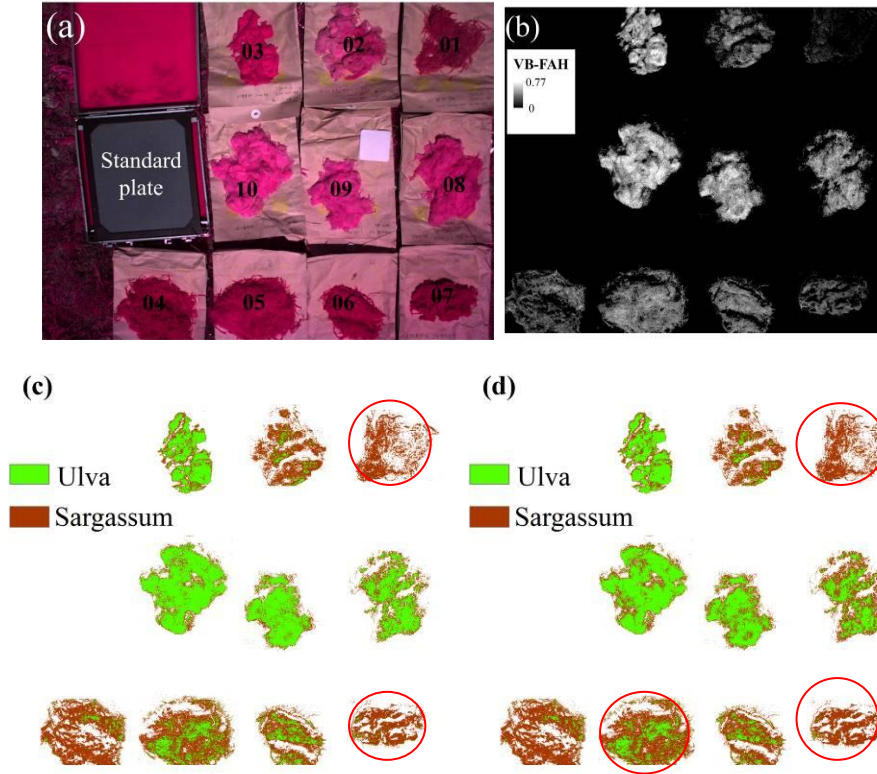


Fig.2. (a) The multi-spectral reflectance image with NIR, Red and Green combination based on the multispectral imager. (b) The macroalgae extraction result by VB-FAH; (c) and (d) are the classification result obtained by the threshold method: (c) T-depth (0.30); (d) VB-FAH (0.44). The sample marked by the red circle is the one with less than 50% accuracy.

Table 2 The accuracy of each sample (%)

		T-depth	VB-FAH
<i>Sargassum</i>	01	99.82↑	99.46
	04	84.02↓	85.55
	05	50.79↑	48.67
	06	52.06↓	53.35
	Mean	71.67↓	71.76
<i>Ulva prolifera</i>	02	22.58↓	29.23
	03	82.02↓	85.82
	07	13.87↑	9.15
	08	79.64↑	70.27
	09	84.81↑	83.15
	10	88.32↑	87.66
	Mean	61.87↑	30.88

Note: ‘↑’ represents that the accuracy of T-depth is higher than that of VB-FAH, and ‘↓’ is the opposite. The formula of calculated accuracy: $A = N_{\text{classify}_i} / N_{\text{total}_i}$, where A is the classification accuracy, N_{classify_i} is the sum of the *Ulva* or *Sargassum* pixels classified correctly of each sample, N_{total_i} is the total number of *Ulva* or *Sargassum* pixels of each sample extracted by the VB-FAH, i is the sample number.

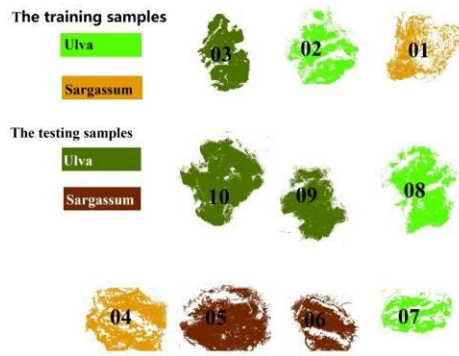


Fig.3. The training samples and the testing ones

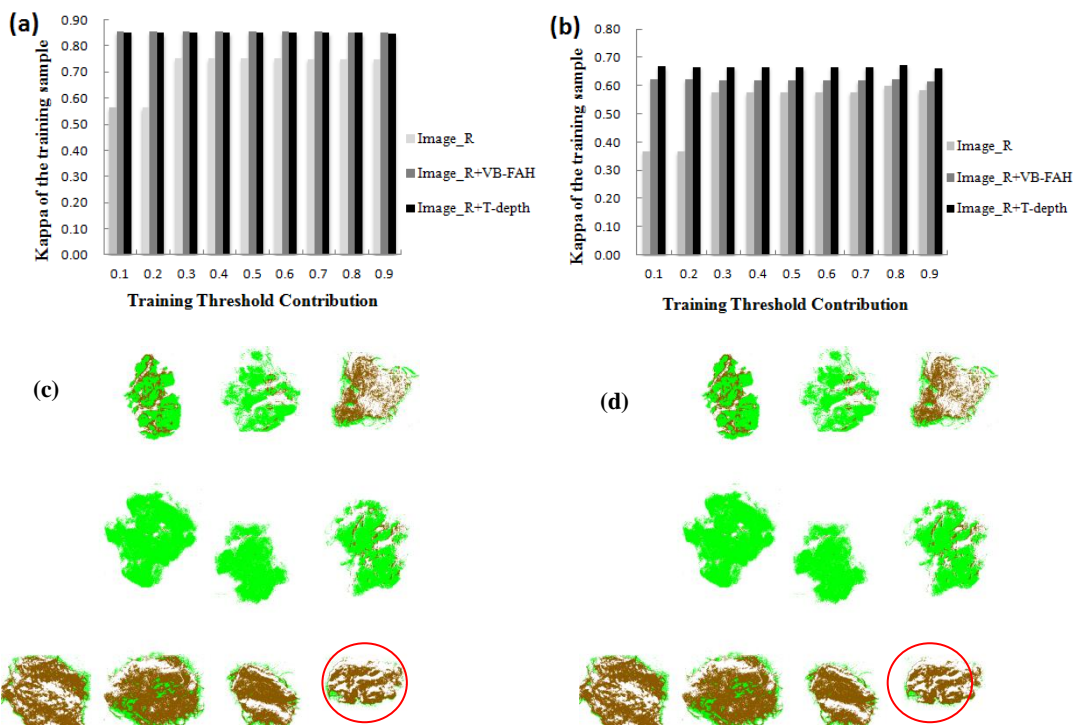


Fig. 4. Comparison of Kappa of neural network classification results. (a) Kappa of the training samples; (b) Kappa of the testing samples. The neural network classification results: (c) Image_R+VB-FAH; (d) Image_R, Image_R+T-depth and Image_R+VB-FAH represents the multispectral reflectance image, the composited image of reflectance and the T-depth and the composited image of reflectance and the VB-FAH, respectively.

参考文献

邢前国, 禹定峰, 娄明静等, 2013. 基于现场光谱的潮滩表层沉积物叶绿素-a 含量遥感模式. 光谱学与光谱分析, 33(8): 2188—2191.

Xing Q G, Hu C 2016. Mapping macrolagal blooms in the Yellow Sea and East China Sea using HJ - 1 and Landsat data: Application of a virtual baseline reflectance height technique. Remote Sensing of Environment, 178: 113—126.

Xing Q G, Guo R H, Wu L L, *et al*, 2017 . High-Resolution satellite observations of a new hazard of "Golden Tides" caused by floating *Sargassum* in Winter in the Yellow Sea. IEEE Geoscience and Remote Sensing Letters.